Electric Power Systems Research 148 (2017) 59–73

Contents lists available at ScienceDirect

Electric Power Systems Research

journal homepage: www.elsevier.com/locate/epsr

# Green Data Centres integration in smart grids: New frontiers for ancillary service provision

Diego Arnone[a], Antonino Barberi[a], Diego La Cascia[b], Eleonora Riva Sanseverino[b], Gaetano Zizzo[b,*]

[a] Engineering Ingegneria Informatica s.p.a. Viale regione Siciliana NO 7275, Palermo 90147, Italy
[b] Università degli Studi di Palermo, Viale delle Scienze Edificio 9, Palermo, Italy

ARTICLE INFO

*Article history:*
Received 5 July 2016
Received in revised form 11 February 2017
Accepted 20 March 2017

*Keywords:*
Green Data Centres
Power system dynamics
Power system management
Spinning reserve
Ancillary services

ABSTRACT

The paper presents a study, conceived within the GEYSER FP7 co-funded European research project, on the ancillary services that Green Data Centres (GDCs) can provide, focusing, in particular, on spinning reserve.

More in detail, the main contribution of the paper is to show how GDCs can be involved in the secondary frequency regulation process of a smart distribution grid, for contrasting the disturbing effects of unexpected variation of the energy production.

With this aim, a real data centre, owned by Engineering S.p.A., is simulated as connected to the Medium Voltage IEEE 14-bus test grid where some RES-based generators are supposed to exist.

Simulations are carried out in order to evaluate the impact of power management actions to be executed by the data centre during under-frequency transients, due to an event of renewable energy facilities power production decrease. During this event, the effects of the spinning reserve provided by the data centre are deeply analysed.



## 1. Introduction

During the last years, a large amount of human and industrial activities have required the recourse to Information and Communication Technology (ICT) leading to an empowerment of Data Centres (DCs) [1,2]. For instance, today in US the energy consumption growth of DCs is ten times bigger than the overall growth of electricity demand [3]; in Europe, instead, DCs requires about 40 TWh (about the 1.5% of the total European energy consumption) [4,5].

In addition, in the last few years, as a result of the increased use of Renewable Energy Sources (RES), such as wind and solar, new challenges have been faced. Indeed, the increase of renewable energy penetration has worsened the management of the power grid [6,7] causing also a spread of the energy prices. In such a context, the opportunity of employing Geen Data Centres (GDCs) in the management of power flows in the grid must be considered [8,9].

GDC is a facility that has a minimal effect on the natural environment. It is entirely built, managed and operated on green computing principles. It provides the same features and capabilities of a typical DC but uses less energy and its design and operation are environmentally friendly. DCs are highly automated and monitored loads and they are characterized by a certain level of demand flexibility [10,11]. For this reason, under well-defined conditions, it is possible to modulate the power loads of the IT equipment [12] as well as the cooling facilities service [9,13].

GEYSER (Green networked data centres as EnergYProSumErs in smaRt city environments) FP7 co-funded European project [14] imagines a scenario in which GDCs are flexible and cooperating "prosumers" able to contribute to the reliability and stability of the power distribution grid.

Empirical studies [15] show that, acting both on the "non IT equipment" [16] and via temperature adjustments (i.e. cooling plants and ventilation facilities, etc.) and therefore without affecting the ICT workload, the 5% of the total load in a DC can be shed in 5 min and the 10% of the load can be shed in 15 min [15,17].

In some cases, a wider range of flexibility can be achieved by acting also on IT workload management by geographically relocating it [18–20]. Moreover, typically DCs have on-site backup generators coupled to large scale energy storage systems [21] in order to ensure the absolute continuity of supply [22], that further increase the flexibility of the installation [23].

* Corresponding author.
*E-mail address:* gaetano.zizzo@unipa.it (G. Zizzo).

http://dx.doi.org/10.1016/j.epsr.2017.03.017
0378-7796/

**Nomenclature**

| | |
|---|---|
| AGC | Automatic generation control |
| AS | Ancillary services |
| DC | Data Centre |
| DFIG | Double field inductor generator |
| DR | Demand Response |
| DQ0 | Direct quadrature zero |
| DSO | Distribution system operator |
| FP | Framework programme |
| FRR | Frequency restoration reserve |
| GDC | Green Data Centre |
| HV | High Voltage |
| ISO | Independent System Operator |
| MV | Medium Voltage |
| PQ | Active and reactive power injected fixed |
| RES | Renewable energy sources |
| RMS | Root mean square |
| RR | Replacement reserve |
| RS | Regulation service |
| SL | Slack voltage value fixed |
| TSO | Transmission system operator |
| TMNSR | Ten Minute Non-Spinning Reserves |
| TMOR | Thirty Minute Operative Reserve |
| TMSR | Ten Minute Spinning Reserves |

This paper presents some main results of the GEYSER research project on this issue. In particular, after describing the ancillary services that a GDC can provide to a smart micro-grid, the paper focuses on spinning reserve provision, presenting some case studies on a real existing DC. More in detail, the main contribution of the paper is to propose the possibility of involving GDCs in the secondary frequency regulation process for contrasting the effects of the unexpected variation of the energy production, in particular in micro-grid with high penetration of RES-based generators.

With this aim, a real data centre located in Pont Saint Martin (PSM), Valle d'Aosta (Italy), owned and operated by Engineering S.p.A., is simulated as connected to the Medium Voltage IEEE 14-bus test grid where some RES-based generators are supposed to exist. Simulations are carried out in order to evaluate the impact of power management actions to be executed by the data centre during under-frequency transients, due to an event of renewable energy facilities power production decrease. During this event, the effects of the spinning reserve that the data centre can provide are deeply analysed.

In the present work, it is assumed that the 14-bus test grid is isolated from the Italian transmission system, and that the secondary frequency regulation is performed only by the PSM Data Centre, thus showing more clearly its effects. It is important to underline that these hypotheses have no influence on the results of the study that leads to broader conclusions valid also for more extended power systems. In fact, when the GDC is considered connected to a not isolated grid, it will be able to participate to the secondary frequency regulation with the same actions, together with the other facilities connected to the Medium Voltage (MV) and High Voltage (HV) systems.

Although the paper does not want to propose a unique solution, the case studies presented in the following clearly show how GDCs can be used for secondary frequency regulation, and the results obtained by simulations can be easily generalized to other critical situations [24].

The paper is structured as follows:

- in Section 2, it is described how GDCs can be integrated in Demand Response programs and how they can be used for providing ancillary services;
- in Section 3, the characteristics of the test network and of the Pont Saint Martin DC are reported and the control system implemented for the secondary regulation is described;
- in Section 4, simulations are performed for three different scenarios (no intervention of the DC, DC loads reduction, DC UPS activation), in order to evaluate the impact of the actions of the GDC during under-frequency transients due to a decrement of the power production by the renewable energy facilities of the micro-grid;
- in Section 5, the results of the simulations are discussed and in Section 6, the conclusions of the work are presented.

## 2. Data Centres and ancillary services

Conventional power plants are fully efficient when their output is a constant amount of power and when they supply the "base load" to electrical grid's users; other power plants, known as peaking plants, change up and down their output to balance the supply with the demand. These plants are less efficient in the conversion of fuel to electricity.

To avoid the use of conventional power plants to cover peak load, cooperation Demand Response (DR) programs between DSO and prosumers could be used [25–27]. DR was conceived as a technique for balancing electricity supply and demand by regulating power consumption of users without impacting on conventional generation plants [28]. Facilities that can modulate their load and their production through energy storage and DR programs may help to increase production and distribution efficiency, cover peak demand, thus relieving the conventional power plants.

The use of DR programs is a crucial point and a key technology that allows the development of "smart electric grids" as shown in Fig. 1.

DR programs aim to increase grid efficiency, while incorporating significant amounts of clean renewable energy sources. They allow to implement a continuous collaboration between prosumers and grid operators in order to optimize power consumption during market-based pricing time [22] or to deal with power variations from not dispatchable RESs [8]. DR programs between DCs and smart grid allows to avoid greenhouse gas (GHG) emissions [29], congestion of the lines and wide recourse to conventional power plant [30]. It can also allow conventional energy producers to obtain cost savings and consequently energy consumers to buy energy at lower prices [30]. DCs are particularly suitable to adopt and benefit from continuous DR programs [31–33]. The power supply and state of IT equipment and cooling systems can indeed be continuously monitored and regulated [9,12]. DCs involved in DR programs can also provide ancillary services to the DSO [34,35] (Fig. 2) contributing, in this way, to a safer management of the power distribution grid [36–38].

The exchange of ancillary services between DC and DSO depends on:

- how quickly DC can change its own load or can activate/regulate its own backup equipment/generators;
- what is the cost for replacing the load or activating the generators;
- what kind of market conditions exploit these services.

The ancillary services that the GDC can offer are: Regulation Services, Thirty Minute Operative Reserve (TMOR), Ten Minute Spinning Reserve (TMSR), Ten Minute Non-Spinning Reserve (TMNSR) [39].

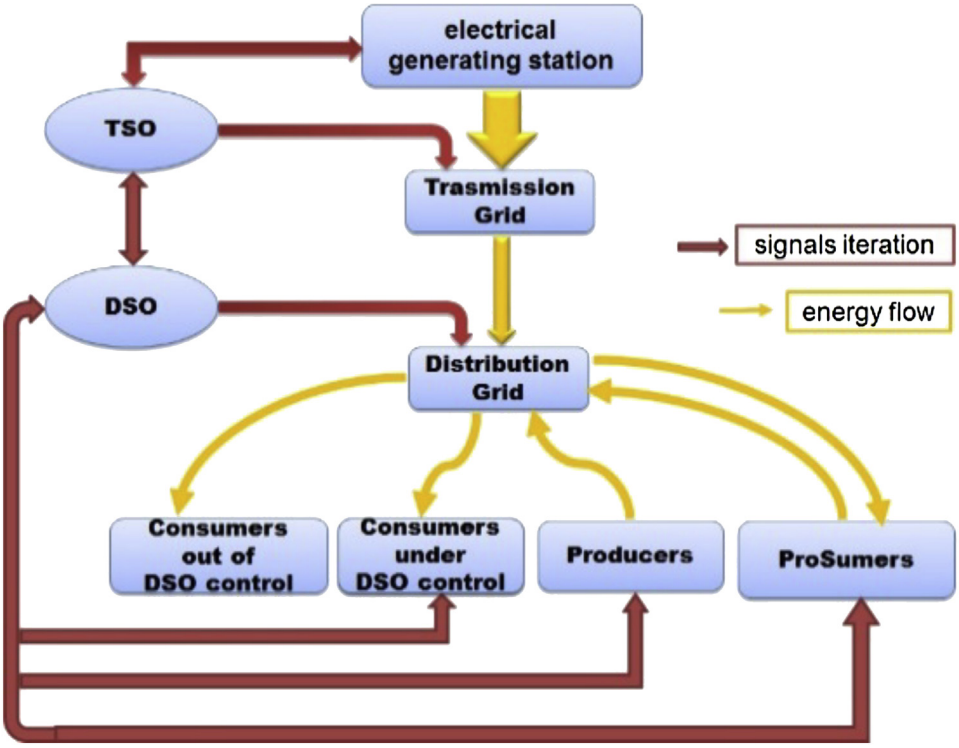


**Fig. 1.** Demand Response power and information flows.

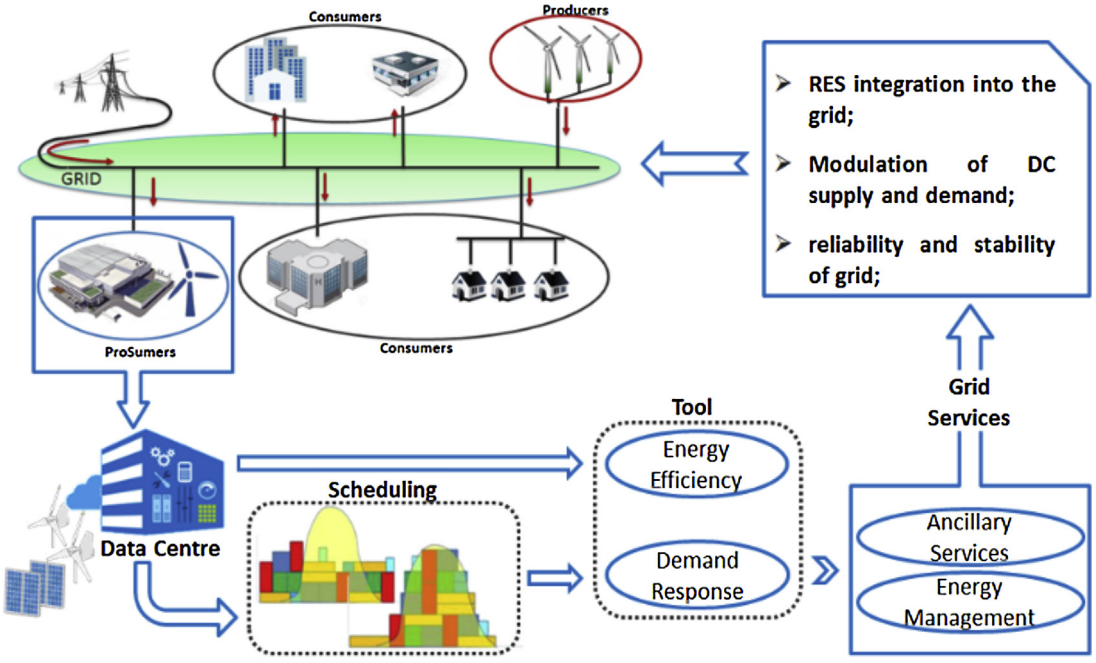


**Fig. 2.** Green Data Centre integration into the Smart Grid.

Spinning reserve, also referred to as "responsive reserve service", is an on-line reserve capacity of the grid for modifying the output power when the frequency increases or decreases. A frequency relay, or a command from the DSO, reduces or disconnects the load. TMOR provides the same service but in a longer time (i.e. signals arrive with 30 min notice typically).

TMNSR is aimed to restore the electrical power system reserves. The adjustment services consist in the reduction or increase of the loads based on control signals coming from the grid [7], contributing to ensure a certain level of power quality. TMSR service is paid more than TMNSR, which is paid more than TMOR. The three mentioned services are defined as "operative reserve of system". The payments for participation in such programs are rather complicated. Such markets are typically operated by Independent System Operator (ISO) [40] for competitive procurement of reserves that are needed to guarantee the secure operation of a competitive electric power system.

The procurement of ancillary services is usually based on acquisitions by means of auctions (simultaneous or not between TMSR-TMNSR services and TMOR services) [41] through a bidding process, both in ancillary services markets, or through bilateral contracts (capacity payments) between ISO and GDC [15,22].

Nevertheless, few works have been reported in scientific literature on the impacts of DR on dynamic performance of power systems, specifically on the load frequency control problem. One of the most significant contribution to the problem can be found in [42], where it is shown that the addition of the DR control loop increases the stability margin of the system and DR effectively improves the system dynamic performance. Another contribution to this issue is given in [43], where the authors present the impact of DR control loop with communication delay in two-area thermal power systems for improvement in frequency deviation profile.

With reference to how secondary frequency control is performed, the authors referred to the technical document "Participation to frequency and frequency-power regulation" [44] by TERNA, the Italian TSO.

Fig. 3 represents the DR frequency control algorithm. More in detail, in Fig. 3 is assumed that a power imbalance occurs in the MV grid, due to the reduction of the power produced by a RES-based generator or to the increase of the load demand.

The frequency control loop, is sensitive to the difference $\Delta f$ between the set-point frequency $f_o$ and the actual frequency f after the primary regulation. The Grid Regulator of the TSO sends a command signal to the DSO. In the considered case, the DSO has an own Grid Regulator, that sends a command signal to the GDC (but also to the other generators, loads and devices taking part to the secondary regulation, as represented in Fig. 1). The GDC varies its electric profile, by acting on its interruptible loads or on its UPSs according to the CEI Standard 0–16, that is the National Technical Rule for the connection of active and passive users to the MV distribution grid [37]. This determines a frequency variation. The regulation operated by the GDC concludes when the GDC's resources have been totally exploited (in this case the regulation is concluded by the TSO) or when the grid frequency reaches the set-point value $f_o$. At the same way, if the installation has a rated power below 100 kW, the secondary control regulation is accomplished according to the CEI Standard 0–21 [45] that is the National Technical Rule for the connection of active and passive users to the LV distribution grid.

## 3. Characteristics of the test system

### 3.1. Test grid

The interaction analysis between the real GDC and the electrical test grid has been carried out by supposing that the Pont Saint Martin DC is connected to the IEEE 14-bus test grid, described in Ref. [46] and suitably modified in order to take into account the main features of the real transmission and distribution systems to which the DC is connected in Valle D'Aosta. The system chosen is able to represents some realistic situations like small islands' distribution systems not connected to the main grid or portion of the distribution grid isolated from the main grid in emergency conditions. The grid topography is shown in Fig. 4, where two different zones are visible: a 132 kV High Voltage area (green-coloured), and a 15 kV Medium Voltage area (red-coloured). The main grid is characterized by:

- 17 buses;
- 7 HV lines and 8 MV lines;
- 2 synchronous machines;
- 7 Yy0 transformers;
- 10 MV loads and 4 HV loads:
- 5 RES-based generator: 2 Doubly Fed Inductor Generators (DFIGs) and 3 photovoltaic (PV) plants.

The parameters of the system are reported in Tables 1–5.

Simulations have been carried out by means of the "NEPLAN Smarter Tools" software [47] which allows to model and analyse electricity, gas, water and heating networks. NEPLAN simulates each component by an equivalent Pi-circuit defined by its positive and zero sequence impedance and admittance. In the simulations a constant model has been assumed for the electric loads.

### 3.2. Pont Saint Martin Data Centre

The power distribution system of the Pont Saint Martin (PSM) DC, represented in Fig. 5, has a redundant layout according to "Tier 4" standard [28].

The PSM DC is connected to the main grid at bus B6. Its own power grid includes:

- 11 buses;
- 2 MV lines (red-coloured);
- 7 LV lines (blue-coloured);
- 3 backup generators with rated active power 1400 kW at $\cos\varphi = 0.8$:
- 4 transformers (a couple per backbone for grid supply redundancy);
- 3 UPS with rated power 800 kVA;
- 7 electrical load centres, including 4 flexible loads and three IT not-interruptible loads (Table 6).

### 3.3. Control system

The study concerns the dynamic analysis of the system with the aim of evaluating the contribution of the PSM GDC during Frequency Restoration Reserve (FRR) or secondary response. In this way, it is possible to evaluate how the DC can participate in the ancillary services delivery and, specifically, in spinning reserve delivery (TMSR, TMOR).

A similar study, considering a 14-bus grid hosting a data centre and a RES plant, has been carried out in Ref. [24]; however, the latter investigates the potential of DC Demand Response as a tool for supporting an efficient load profile coverage in presence of a large scale RES installation.

The supply of ancillary services to the grid allows a higher level of integration of DCs in the smart grid [41] that paves the way towards the definition of new market scenarios and new business models for DCs [40].

In this work, has been investigated how PSM DC contributes to the management of the intermittency of the RES generators, in case of:

1. wind farm production decrease;
2. PV production decrease

In order to evaluate the different contribution that a real DC can give to the grid when a significant and instant decrease of energy production occurs, the dynamic analysis of the grid frequency trend has been carried out in three different scenarios:

a) scenario a: no intervention of the GDC;
b) scenario b: GDC load reduction;
c) scenario c: GDC UPS activation.

In the above scenarios, the frequency has been detected at bus B6 and the grid has been supposed iso-frequential.

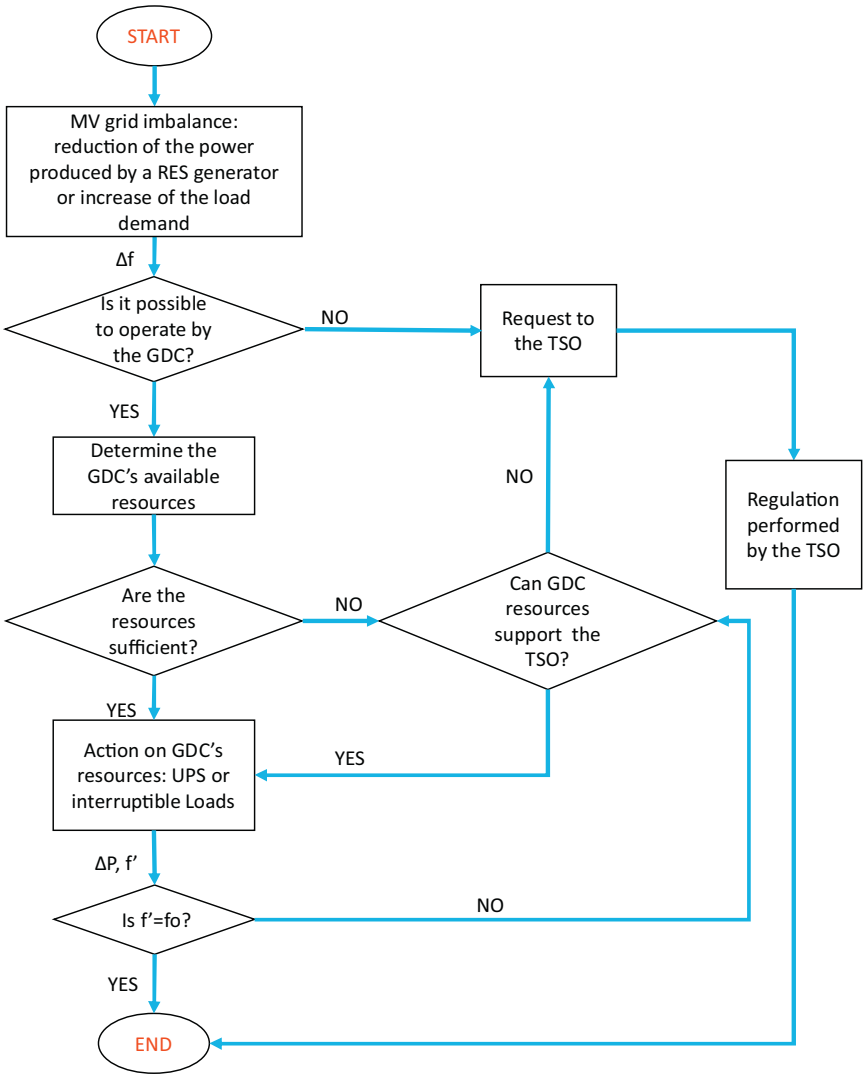


**Fig. 3.** Flow chart of the DR frequency control algorithm.

**Table 1**
Main grid lines.

| From bus- to bus | Line [km] | Ur [kV] | r1 [Ω/km] | x1 [Ω/km] | b1 [μS/km] | g1 [μS/km] | r0 [Ω/km] | x0 [Ω/km] | b0 [μS/km] |
|---|---|---|---|---|---|---|---|---|---|
| B1–B2 | 2.0 | 132 | 0.084 | 0.406 | 2.71 | 0.01 | 0.252 | 1.218 | 8.13 |
| B1–B2 | 2.0 | 132 | 0.084 | 0.406 | 2.71 | 0.01 | 0.252 | 1.218 | 8.13 |
| B1–B5 | 3.0 | 132 | 0.084 | 0.406 | 2.71 | 0.01 | 0.252 | 1.218 | 8.13 |
| B2–B5 | 1.5 | 132 | 0.084 | 0.406 | 2.71 | 0.01 | 0.252 | 1.218 | 8.13 |
| B2–B4 | 3.0 | 132 | 0.084 | 0.406 | 2.71 | 0.01 | 0.252 | 1.218 | 8.13 |
| B2–B3 | 3.0 | 132 | 0.084 | 0.406 | 2.71 | 0.01 | 0.252 | 1.218 | 8.13 |
| B3–B4 | 2.0 | 132 | 0.084 | 0.406 | 2.71 | 0.01 | 0.252 | 1.218 | 8.13 |
| B4–B5 | 1.5 | 132 | 0.084 | 0.406 | 2.71 | 0.01 | 0.252 | 1.218 | 8.13 |
| B9–B10 | 0.1 | 15 | 0.124 | 0.11 | – | – | 0.372 | 0.330 | – |
| B9–B14 | 0.4 | 15 | 0.124 | 0.11 | – | – | 0.372 | 0.330 | – |
| B10–B11 | 0.3 | 15 | 0.124 | 0.11 | – | – | 0.372 | 0.330 | – |
| B6–B11 | 0.4 | 15 | 0.124 | 0.11 | – | – | 0.372 | 0.330 | – |
| B6-B13 | 0.5 | 15 | 0.124 | 0.11 | – | – | 0.372 | 0.330 | – |
| B6–B12 | 0.6 | 15 | 0.124 | 0.11 | – | – | 0.372 | 0.330 | – |
| B12–B13 | 0.5 | 15 | 0.124 | 0.11 | – | – | 0.372 | 0.330 | – |
| B13–B14 | 0.3 | 15 | 0.124 | 0.11 | – | – | 0.372 | 0.330 | – |

**Table 2**
Main grid synchronous machines.

| Name | Sr [MVA] | Ur [kV] | cosϕ | xd sat% | xd'sat% | xd"sat% | x(2)% | x(0)% | Ufmax/Ur | LF Type | P Gen [MW] | Q Gen [MVAR] | H. [s] | D. [MW/Hz] | Xd'% |
|---|---|---|---|---|---|---|---|---|---|---|---|---|---|---|---|
| GEN1 | 12 | 10 | 0.80 | 116 | 27 | 20 | 19 | 7 | 1.3 | Slack bus | – | – | 5 | 1 | 5 |
| GEN3 | 12 | 10 | 0.80 | 116 | 27 | 20 | 19 | 7 | 1.3 | PQ Node | 9 | 7 | 5 | 1 | 5 |

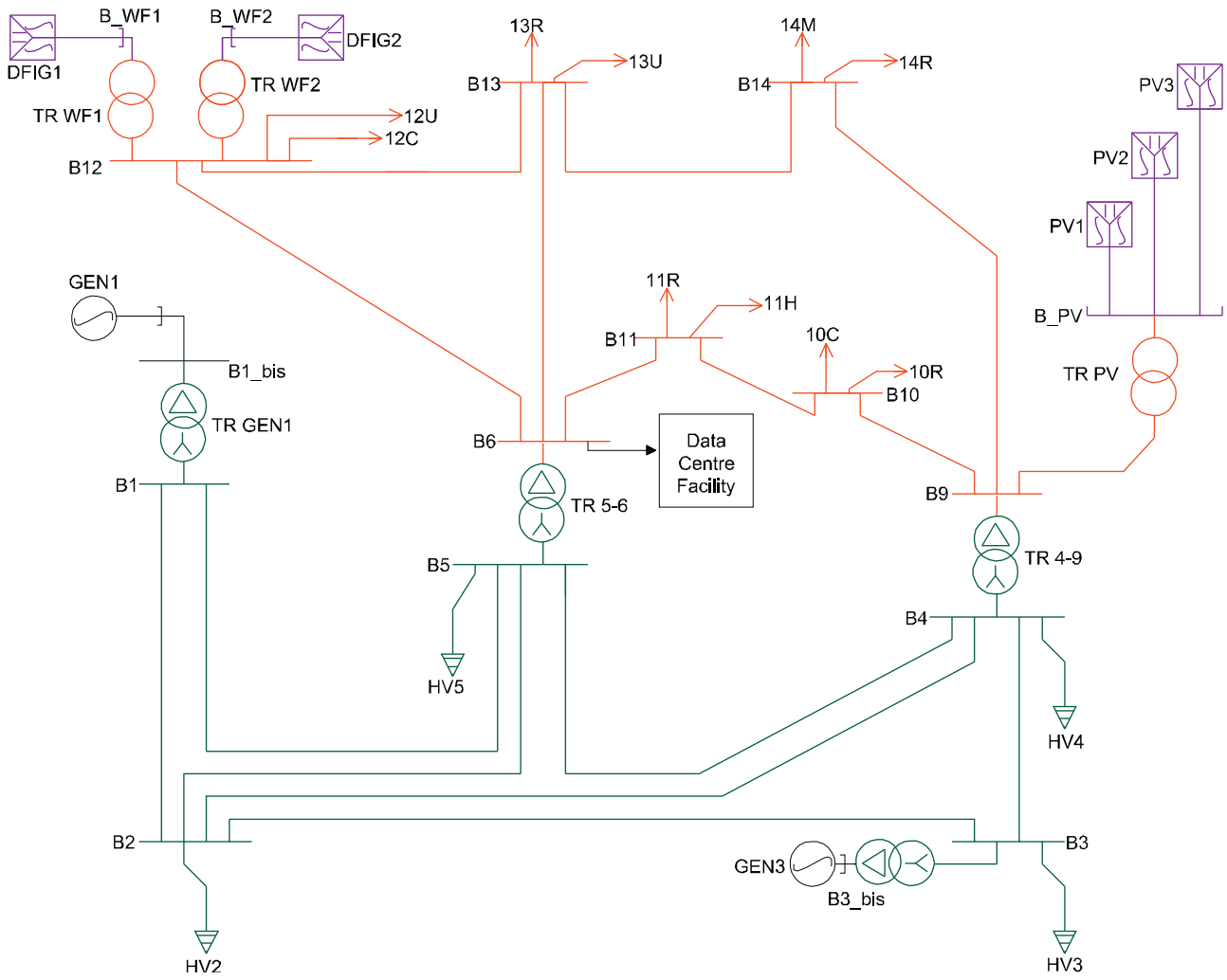


**Fig. 4.** Test grid in NEPLAN. (For interpretation of the references to colour in the text, the reader is referred to the web version of this article.)

**Table 3**
Transformers.

| TR | S [MVA] | $Ur^1$ [kV] | $Ur^2$ [kV] | Ukr (1)% | uRr (1)% | Ukr (0)% | uRr (0)% | Earth Prim | $R_E^1$ [Ω] | $X_E^1$ [Ω] | Earth sec. | $R_E^2$ [Ω] | $X_E^2$ [Ω] | Tap | $I_0$% | Pfe [kW] |
|---|---|---|---|---|---|---|---|---|---|---|---|---|---|---|---|---|
| TR 5-6 | 10.00 | 132 | 15 | 13 | 0.65 | 13 | 1.95 | Direct | 0.1 | 0 | Peter. | 0 | 0 | ±15 | 1 | 14 |
| TR 4-9 | 10.00 | 132 | 15 | 13 | 0.65 | 13 | 1.95 | Direct | 0.1 | 0 | Peter. | 0 | 0 | ±15 | 1 | 14 |
| TR G1 | 12.00 | 132 | 10 | 13 | 0.65 | 13 | 1.95 | Direct | – | – | Peter. | – | – | ±15 | 1 | 14 |
| TR G2 | 12.00 | 132 | 10 | 13 | 0.65 | 13 | 1.95 | Direct | – | – | Peter. | – | – | ±15 | 1 | 14 |
| TR PV | 3.00 | 15 | 0.69 | 8 | 0.75 | 8 | 2.25 | Direct | – | – | Peter. | – | – | ±15 | 0.4 | 6.6 |
| TR_WF1 | 3.00 | 15 | 0.69 | 8 | 0.75 | 8 | 2.25 | Direct | – | – | Peter. | – | – | ±15 | 0.4 | 6.6 |
| TR_WF2 | 3.00 | 15 | 0.69 | 8 | 0.75 | 8 | 2.25 | Direct | – | – | Peter. | – | – | ±15 | 0.4 | 6.6 |

**Table 4**
Loads.

| Bus | Load | Type | Ur [kV] | Ac [kVA] | Pc [kW] | Qc [kVAR] |
|---|---|---|---|---|---|---|
| B10 | 10R | Residential | 15 | 175.00 | 157.50 | 76.281 |
| B10 | 10C | Commercial | 15 | 170.00 | 144.50 | 89.553 |
| B11 | 11H | Hospital | 15 | 173.00 | 147.05 | 91.133 |
| B11 | 11R | Residential | 15 | 175.00 | 157.5 | 76.281 |
| B12 | 12C | Commercial | 15 | 170.00 | 144.50 | 89.553 |
| B12 | 12U | Office | 15 | 180.00 | 153.00 | 94.821 |
| B13 | 13R | Residential | 15 | 175.00 | 157.50 | 76.281 |
| B13 | 13U | Office | 15 | 180.00 | 153.00 | 94.821 |
| B14 | 14R | Residential | 15 | 175.00 | 157.50 | 76.281 |
| B14 | 14M | Hotel | 15 | 115.00 | 103.50 | 50.127 |
| B2 | HV2 | – | 132 | 1044.00 | 939.60 | 455.069 |
| B3 | HV3 | – | 132 | 1044.00 | 939.60 | 455.069 |
| B4 | HV4 | – | 132 | 1044.00 | 939.60 | 455.069 |
| B5 | HV5 | – | 132 | 1044.00 | 939.60 | 455.069 |

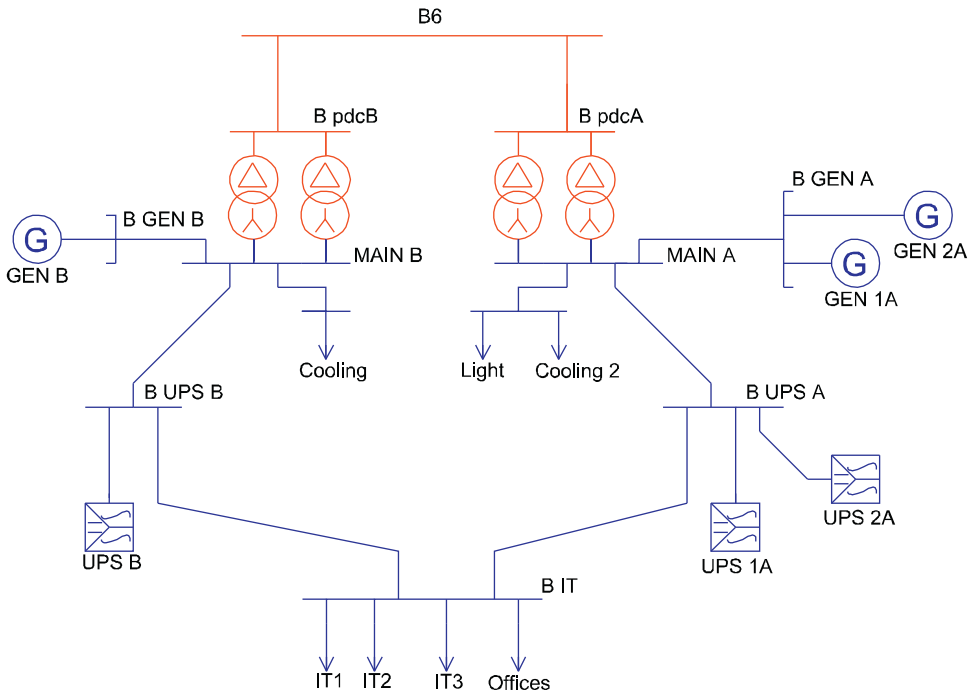


**Fig. 5.** Pont Saint Martin DC single line diagram in NEPLAN. (For interpretation of the references to colour in the text, the reader is referred to the web version of this article.)

**Table 5**
RES generators.

| RES generator | P [kW] | Q [kVAR] |
|---|---|---|
| PV 1 | 450 | 135 |
| PV 2 | 450 | 135 |
| PV 3 | 100 | 10 |
| DFIG 1 | 1600 | 1200 |
| DFIG 2 | 1600 | 1200 |

Starting from the above-listed scenarios, the simulated control system in Fig. 6, has been adopted for simulating the primary frequency regulation at the TSO level as well as the secondary regulation at the DSO level.

The control system is composed of two parts:

- the blocks in the upper part of Fig. 6 (in blue) simulate the TSO control action during the primary frequency regulation;
- the blocks in the lower part of Fig. 6 (in yellow) simulate the DC control action during the secondary frequency regulation.

The dynamic simulation has been carried out during a day of July day at 12:00. Before applying disturbances (a sudden power decrease) standard operating conditions for loads, RES power plants and backup plants have been assumed.

The calculation parameters for the solver are:

- type of simulation RMS-DQ0 (Root Mean Square—Direct Quadrature axis). Transient stability or electromechanical simulation with DQ0 models [47]. This simulation mode should be used for RMS simulations of balanced systems with balanced faults (e.g. 3-phase fault, simultaneous phases' detachment, etc.);
- simulation time step: $0.5 \times 10^{-6}$ s;
- maximum simulation time: 900 s.

### 3.3.1. *Primary frequency control/regulation*

The primary frequency regulation/control consists of an automatic response operated through the control of generation. In the present work, the grid frequency set-point value is selected according to Ref. [48] and is equal to 50 Hz.

This control starts with no delay after the disturbance occurrence and it is carried out by 30 s. At the end of the regulation, the grid frequency value must be in the range $49.9 \div 50.1$ Hz [49].

In order to investigate the behaviour of the GDC during secondary regulation, the primary control has been simulated in a simple way by using the HV loads zone shift control [46] instead of a classical speed governor. In this way, in the following a not null frequency steady-state error is obtained at the end of the primary regulation that allows to simulate the GDC participation to the secondary regulation. In any case, the way used for simulating the primary frequency control is not relevant for the aim of the work, given that the GDC takes part only to the secondary regulation.

In this control system, the grid frequency value is measured at bus *B6* and generates the signal ($u_1$); the latter is compared to three

**Table 6**
PSM loads.

| Bus | Ur [kV] | Power [kVA] | Pc [kW] | Qc [kVAR] | −5%Pc [kW] | −10%Pc [kW] |
|---|---|---|---|---|---|---|
| Lighting | 0.4 | 16.77 | 15 | 7.50 | 0.75 | 1.50 |
| Cooling | 0.4 | 95.97 | 86 | 42.60 | 4.30 | 8.60 |
| Cooling 2 | 0.4 | 196.79 | 177 | 86.00 | 8.85 | 17.70 |
| IT1 | 0.4 | 340.13 | 306 | 148.50 | – | – |
| IT2 | 0.4 | 339.91 | 306 | 148.00 | – | – |
| IT3 | 0.4 | 341.96 | 308 | 148.58 | – | – |
| Offices | 0.4 | 38.89 | 35 | 16.95 | 1.75 | 3.50 |

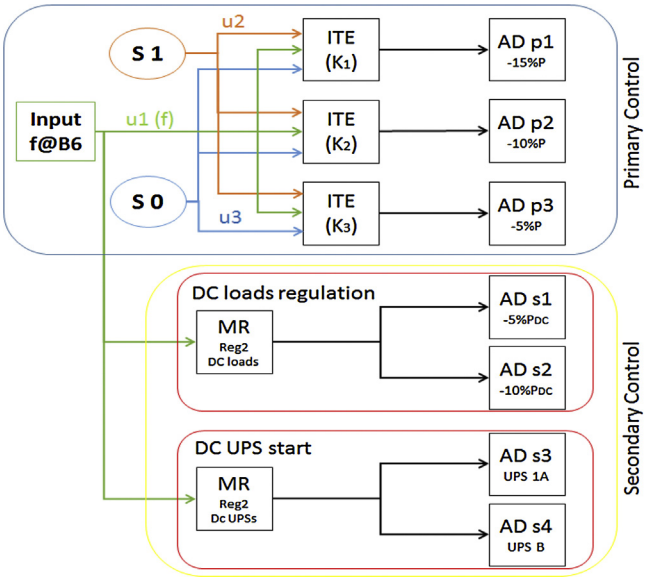


**Fig. 6.** Frequency control System implemented in NEPLAN. (For interpretation of the references to colour in the text, the reader is referred to the web version of this article.)

**Table 7**
Power shifting grid loads.

| Load | Delay red1 [s] | Red1. f < 49.89%Pn | Delay red2[s] | Red2. f < 49.875%Pn | Delay red3[s] | Red3. f < 49.625%Pn |
|---|---|---|---|---|---|---|
| HV2 | 1 | 5% | 4 | 10% | 8 | 15% |
| HV3 | 1 | 5% | 4 | 10% | 8 | 15% |
| HV4 | 1 | 5% | 4 | 10% | 8 | 15% |
| HV5 | 1 | 5% | 4 | 10% | 8 | 15% |

different frequency thresholds $K_i$ (i = 1, 2, 3) in a logical block "*If-Then-Else (ITE)*".

The *ITE* blocks (Fig. 6) are also equipped with two constant signals:

- ○ $u_2$ equal to 1 (generated by the block "*Source (S1)*");
- ○ $u_3$ equal to 0 (generated by the block "*Source (S0)*").

Depending on $u_1$ value, the *ITE* block gives as output the value $u_2$ or the value $u_3$.

According to Italian TSO [45], three logical blocks with different $K_i$ constant have been considered:

- K1 = 49.850;
- K2 = 49.875;
- K3 = 49.890.

When the grid frequency is lower than $K_i$, the corresponding "*i*" function block "*Active Disturbance (AD)*" acts on the loads reducing the power absorbed by them. The power reduction depends on the frequency disturbances shown in Table 7.

### 3.3.2. Secondary frequency/power control/regulation

The secondary frequency/power regulation/control starts after the primary regulation or during its final time frame and is, usually, carried out within 15 min (900 s).

In secondary regulation, the DC modulates its energy consumption. The control is carried out by means of a function block "*Minimum Relay (MR)*", that senses the grid frequency values at bus B6. The function block works with a binary logic as shown in Fig. 7.

$$y_1 = \begin{cases} highstatus\ \text{“1”}\ u_1 \le K_1 = 50.0\ \text{Hz} \\ lowstatus\ \text{“0”}\ u_1 \ge K_2 = 50.1\ \text{Hz} \end{cases} \quad (1)$$

When the grid frequency is lower than 50 Hz the corresponding "*i*" function block "*Active Disturbance (AD si)*" (i = 1–4) acts on the DC plants.

With regard to the way chosen for implementing the secondary control of the GDC some more considerations are due. Although, a real accurate setting of the minimum relay has been assumed in the present work, the actual secondary frequency control scheme used in the electric power system is the automatic generation control (AGC).

Nevertheless, existing DCs have not AGC while one of the aspect of the GEYSER research project is to investigate what kind of ancillary services can be provided by the existing DCs using the devices already available at the DC installation site, without including important modifications in the installation. Indeed, the DC core business is to sell ICT services whereas the possibility of collaborating with the grid is a secondary task related to its integration in future smart-grid, that must be threaten a secondary task and considering all the possible risks for the service offered by the DC. For this reason in this work the secondary regulation is done using the minimum relay and not the AGC.

The DC can perform the secondary frequency regulation in two different ways:

- ○ by acting on DC loads energy consumption;
- ○ by acting on DC UPS activation.

In the first case, the DC reduces the power consumption of its loads as shown in Table 8.

When the grid frequency is lower than 50 Hz the corresponding "*i*" function block "*Active Disturbance (AD s1)*" acts on the DC loads, reducing the power absorbed by them. At the end of the reduction, if the value of frequency is still lower than 50 Hz, another function block "*Active Disturbance (AD s2)*" turns on and reduces the loads again. When the grid frequency gets to 50.1 Hz the blocks *AD s1*

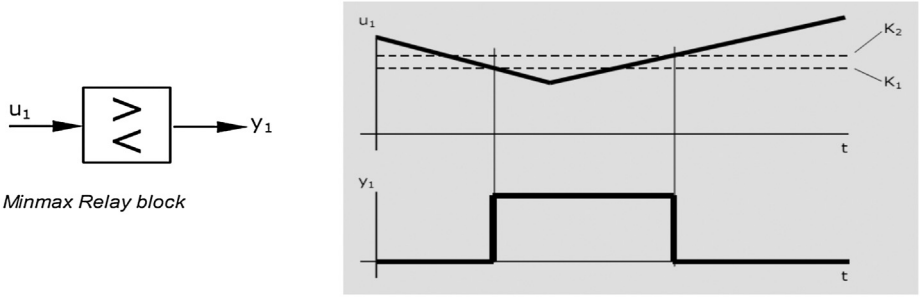


(a) NEPLAN MinMax Relay block; (b) NEPLAN Function Block Minimum Relay.

**Fig. 7.** (a) NEPLAN MinMax Relay block; (b) NEPLAN Function Block Minimum Relay.

**Table 8**
PSM modulated loads power shifting and time delay.

| Load | Delay red1 [s] | Red.5% Pc [kW] | Delay red2 [s] | Red.10% Pc [kW] |
|---|---|---|---|---|
| Lighting | 20 | 1.50 | 240 | 0.75 |
| Cooling | 60 | 8.60 | 720 | 4.26 |
| Cooling x2 | 120 | 17.70 | 600 | 8.60 |
| Offices | 30 | 3.50 | 420 | 1.70 |

**Table 9**
PSM UPSs power output and time relay.

| Name | Delay [s] | Active power output %P | Reactive power output %Q |
|---|---|---|---|
| UPS 1A | 20.00 | 20.00% | 20.00% |
| UPS B | 30.00 | 20.00% | 20.00% |

**Table 10**
Total loads in static steady-state analysis.

| Load | P [kW] | Q [kVAR] |
|---|---|---|
| Area HV loads | 9758.40 | 1820.28 |
| Area MV loads | 1475.55 | 815.13 |
| Area DC loads | 1073.85 | 598.13 |

**Table 11**
Total RES generation in static steady-state analysis.

| Generator | P [kW] | Q [kVAR] |
|---|---|---|
| PV 1 | 450 | 135 |
| PV 2 | 450 | 135 |
| PV 3 | 100 | 10 |
| DFIG 1 | 1600 | 1200 |
| DFIG 2 | 1600 | 1200 |

and *AD s2* switch off; the frequency regulation takes place into the range 49.9 ÷ 50.1 Hz.

In the second case, the DC supplies some loads through its UPSs as shown in Table 9.

In this case, the two function blocks "*Active Disturbance (AD s3)*" and "*Active Disturbance (AD s4)*" receive a signal from the function block "*Minimum Relay (MR) DC UPSs start*"; the functioning is analogous to functioning of "*DC loads regulation*" blocks *AD s1* and *AD s2*; these blocks drive the UPSs start.

In order to allow the primary control regulation action, in *AD s3* and *AD s4*, a delay of 20 s has been set up after that the grid disturbance occurs. In the DCs, the UPSs ensure the absolute continuity of the supply, so it has been supposed to employ only 2 UPSs at 20% of their capability Table 10.

**Table 13**
Scenario A areas power flow.

| From area | To area | P [MW] | Q [MVAR] |
|---|---|---|---|
| Area MV | Area DC | 1.252 | 0.699 |
| Area MV | Area HV | 10.423 | 1.858 |

## 4. Case study

### 4.1. Steady-state—load flow

A preliminary step of the study concerns the steady-state analysis of the system composed by the grid and the PSM GDC. The aim is to evaluate the load flow in two different cases: GDC connected to the grid, GDC in islanding operation.

The load flow calculation in both scenarios has been performed by using the standard operating condition. The calculation method used is the "Extended Newton-Raphson" (convergence mismatch 0.001 and maximum number of iterations 50). The total loads required and the total generation from renewable energy sources are respectively reported in Tables 10 and 11.

#### 4.1.1. PSM Data Centre connected to the grid

In this scenario, the DC generation sets are turned off and the DC loads are entirely supplied by grid. The load flow converged after three iterations and the power values for each area are shown in Table 12.

The power flow between MV Area and DC Area and the power flow between HV Area and MV area are shown in Table 13.

The values in Table 10 show that the energy production from the RES-based generators connected to the MV grid is about 36% greater than the sum of the MV and DC loads, so a reverse flow from MV area to HV area occurs.

#### 4.1.2. PSM Data Centre islanding operation

In this case the PSM DC is disconnected from the test grid. The DC generating sets are turned on and supply all the DC loads. Generators *GEN B* and *GEN 1A* have been used as active and reactive fixed power generators (PQ), while generator *GEN 2A* has been set

**Table 12**
Load flow results for Scenario A.

| | $P_{load}$ [MW] | $Q_{load}$ [MVAR] | $P_g$ [MW] | $Q_g$ [MVAR] | $P_{RES}$ [MW] | $Q_{RES}$ [MVAR] | ΔP [MW] | ΔQ [MVAR] |
|---|---|---|---|---|---|---|---|---|
| Area HV | 10.277 | 0.361 | 2.481 | 2.41 | 0 | 0 | 0.146 | 1.497 |
| Area MV | 1.476 | 0.815 | 0 | 0 | 4.2 | 2.71 | 0.008 | 0.007 |
| Area DC | 1.233 | 0.599 | 0 | 0 | 0 | 0 | 0.019 | 0.101 |
| Total | 12.986 | 1.775 | 2.481 | 2.41 | 4.2 | 2.71 | 0.214 | 1.886 |

**Table 14**
Load flow results for Scenario B.

| | $P_{load}$ [MW] | $Q_{load}$ [MVAR] | $P_g$ [MW] | $Q_g$ [MVAR] | $P_{RES}$ [MW] | $Q_{RES}$ [MVAR] | ΔP [MW] | ΔQ [MVAR] |
|---|---|---|---|---|---|---|---|---|
| Area HV | 11.516 | 0.586 | 9 | 0.7 | 0 | 0 | 0.158 | 1.723 |
| Area MV | 1.476 | 0.815 | 0 | 0 | 4.2 | 2.71 | 0.009 | 0.008 |
| Area DC | 1.233 | 0.599 | 1.249 | 0.683 | 0 | 0 | 0.016 | 0.084 |
| Total | 14.224 | 2 | 14.45 | 4.093 | 4.2 | 2.71 | 0.224 | 2.092 |

**Table 15**
Scenario B areas power flow.

| From area | To area | P [MW] | Q [MVAR] |
|---|---|---|---|
| Area DC | Area MV | 0 | 0 |
| Area MV | Area HV | 11.674 | 2.309 |

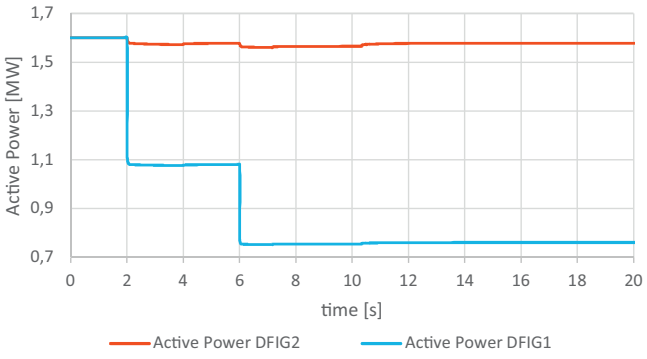


**Fig. 8.** DFIG1 and DFIG2 produced active power.

as a slack bus generator (SL). In this situation, *GEN B* and *GEN 1A* supply entirely the DC, while *GEN 2A* sets the voltage value for the DC grid (*U open.* 100% of rated grid voltage $U_r$) (Table 14).

The load flow converged after 4 iterations and the power values for each area are shown in Table 11.

The power flow between MV Area and DC Area and the power flow between HV Area and MV area are shown in Table 15.

There is no power exchange between MV Area and DC Area. Furthermore, the power flow from MV Area to HV Area has increased. Indeed, in this scenario, when the DC is not connected to the MV grid, the RES energy production is about twice the MV loads demand.

**Table 16**
DFIG shedding production.

| Time | $\Delta P_{gen}$ | $\Delta Q_{gen}$ |
|---|---|---|
| $t_0 = 2$ s | −30% | −30% |
| $t_1 = 6$ s | −20% | −20% |

### 4.2. Dynamic analysis—case 1: DFIG power decrease

In order to evaluate the contribution given by the DC, an instant reduction of the power produced by a wind farm has been supposed to occur [47]. The reduction is related to wind generator DFIG1 and it happens in two time steps as shown in Table 16.

The other components (load, RES, power plant, and DC) continue to work with the same behaviour. The DFIGs power reduction is shown in Fig. 8. The reactive power is supposed to have the same trend of the active power.

#### 4.2.1. Scenario 1a—DC secondary regulation off

In this scenario the DC does not participate in secondary regulation. The primary control is operated in 15 s after the disturbance, therefore the simulation lasts 20 s.

In the connection lines between nodes *B6* and *B pdcA* (line L5-DC_A) and *B pdcB* (line L5-DC_B) the power flow decreases by 30.3 kW as shown in Fig. 9 (this is due to the primary energy/loads regulation effect). The grid frequency trend is shown in Fig. 10.

Once primary regulation concludes and the new steady-state is achieved, the frequency is equal to 49.98 Hz with an error of 0.02 Hz. This result has been used to get a comparison to the results obtained in Scenarios 1b and 1c.

#### 4.2.2. Scenario 1b—DC secondary regulation by loads

In this scenario the DC participates to the secondary frequency/energy regulation by modulating its own few loads. The

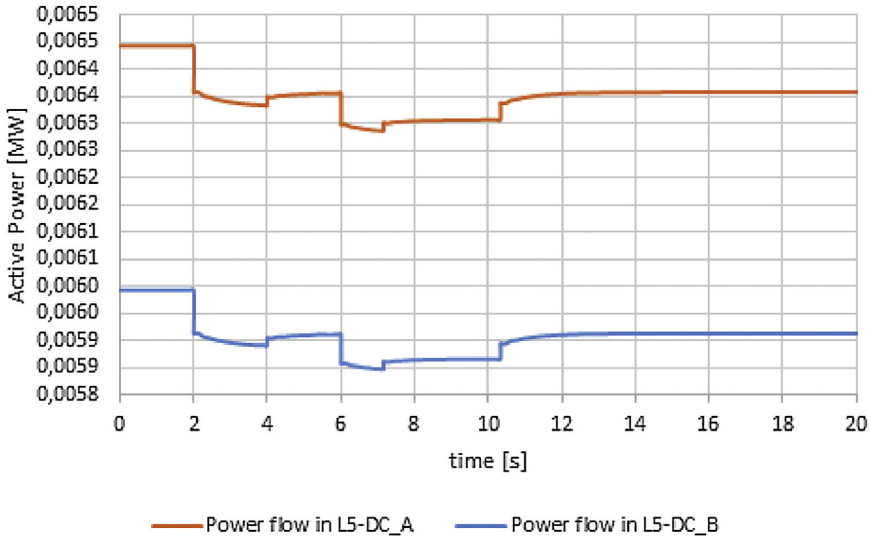


**Fig. 9.** Power flow in the DC lines without DC secondary regulation in scenario 1a.

**Table 17**
Power reduction of the DC loads.

| Offices load reduction [kW] | Cooling load reduction [kW] | Cooling 2 load reduction [kW] | Lighting load reduction [kW] |
|---|---|---|---|
| 2.866 | 8.344 | 17.159 | 1.243 |

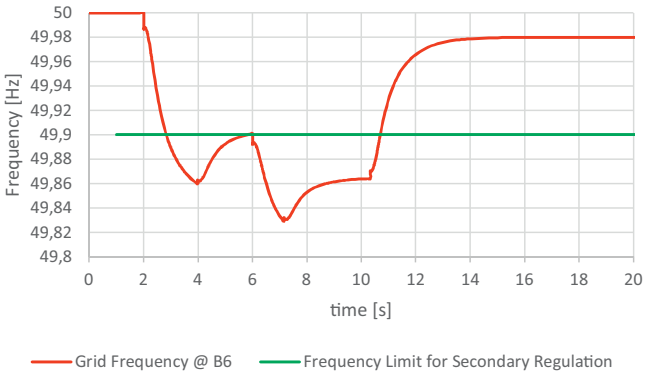


**Fig. 10.** Frequency trend at bus B6 in Scenario 1a.

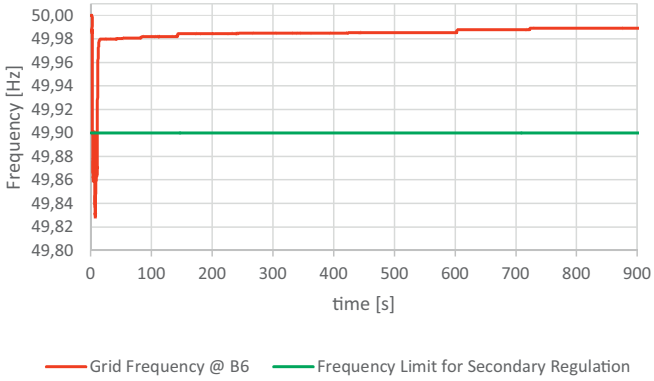


**Fig. 12.** Frequency trend at bus B6 in Scenario 1b.

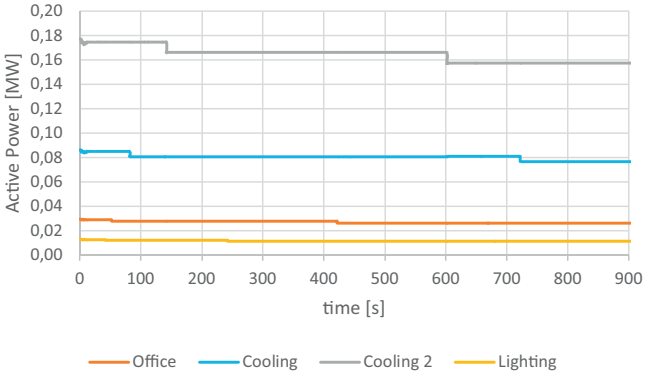


**Fig. 11.** DC loads power reduction in Scenario 1b.

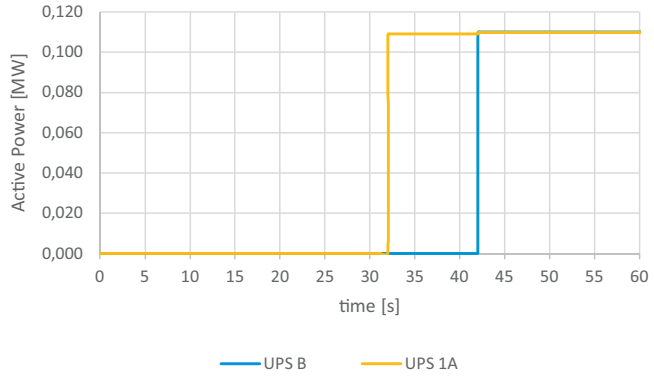


**Fig. 13.** Data centre UPS power supply.

**Table 18**
ΔP in connection line for scenario 1b.

| ΔP in L 5-DC_A [kW] | ΔP in L 5-DC_B [kW] | ΔP tot in L DC [kW] |
|---|---|---|
| 25 | 20 | 45 |

**Table 19**
ΔP in connection line for scenario 1c.

| ΔP L DC_A [kW] | ΔP L DC_B [kW] | ΔP tot L DC [kW] |
|---|---|---|
| 109.9 | 110.0 | 219.9 |

modulation is done in different steps and lasts several minutes, therefore simulation time is 900 s.

Both the function blocks, *"AD s1" and "AD s2"* act on the DC specific loads and reduce the power absorbed by them as reported in Table 17

The power trend is shown in Fig. 11. In the connection line L 5-DC_A and L 5-DC_B the power flow decreases of 45 kW as shown in Table 18.

Once the secondary regulation transient state finished, the frequency is 49.989 Hz with an error of about 0.0108 Hz (0.022% $f_n$) as shown in Fig. 12.

#### 4.2.3. Scenario 1c—DC secondary regulation by UPS

In this scenario the DC participates to the secondary frequency/energy regulation by switching on the UPS devices.

The *Active Disturbance* function block turns on and brings UPS energy delivery to power levels reported in Fig. 13. The action lasts about 40 s, therefore the simulation time is 60 s. In the connection line L 5-DC_A and L 5-DC_B the power flow decreases by 219.9 kW as shown in Table 19.

**Table 20**
PV2 shedding production.

| Time | $\Delta P_{gen}$ | $\Delta Q_{gen}$ |
|---|---|---|
| $t_0 = 2$ s | −25% | −25% |
| $t_1 = 6$ s | −25% | −25% |

After the secondary regulation, the grid frequency is 50.0456 Hz and the error is about −0.0456 Hz (−0.091% $f_n$) as shown in Fig. 14.

### 4.3. Dynamic analysis—case 2: PV power decrease

Another disturbance that can occur is a sudden reduction of the power produced by a PV field. The reduction is related to the photovoltaic field PV2 and it is assumed to happen in two time steps as shown in Table 20.

The other components (load, RES, power plant, and DC) continue to work in the same conditions as before the disturbance. The PV2 power reduction is shown in Fig. 15.

**Table 21**
Power reduction of DC loads in Scenario 2b.

| Offices load reduction [kW] | Cooling load reduction [kW] | Cooling 2 load reduction [kW] | Lighting load reduction [kW] |
|---|---|---|---|
| 3.0136 | 8.776 | 18.047 | 1.308 |

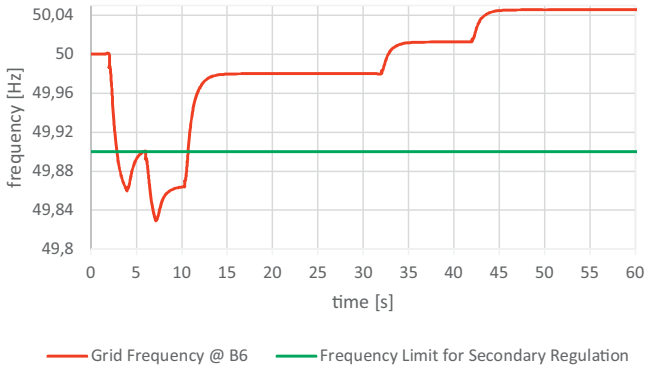


**Fig. 14.** Frequency trend at bus B6 with secondary regulation by data centre UPSs.

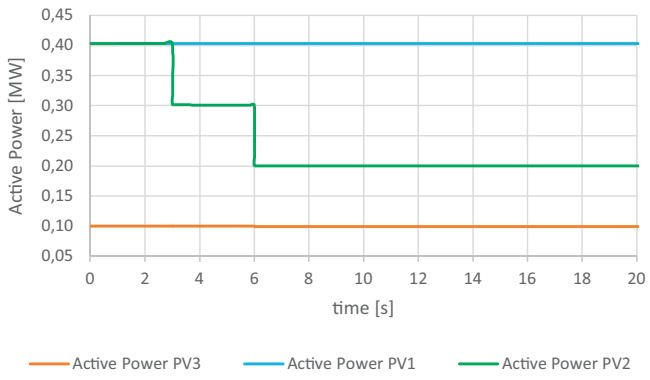


**Fig. 15.** Active power produced by PV1, PV2 and PV3.

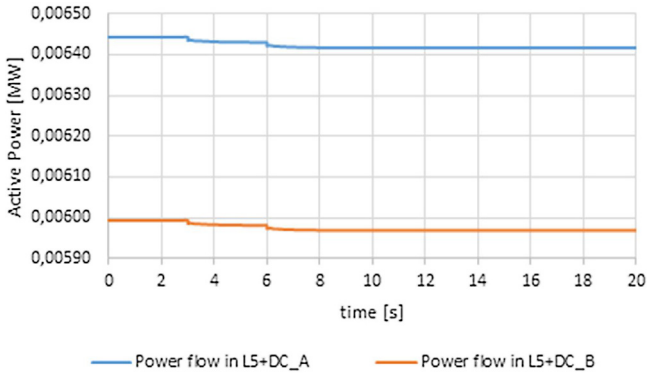


**Fig. 16.** Power flow in the DC lines without DC secondary regulation in Scenario 2a.

In this case, the primary regulation control is not activated because the frequency value is not below 49.9 Hz. Therefore, the grid frequency regulation is performed only by the DC facility during the secondary regulation.

*4.3.1. Scenario 2a—DC secondary regulation off*

In this scenario the DC does not participate to the secondary regulation. The simulation lasts 20 s. In the connection line L 5-DC_A and L 5-DC_B the power flow decreases as shown in Fig. 16, as a consequence of the modified power flows and of the voltage variation in the test grid. The grid frequency trend is shown in Fig. 17.

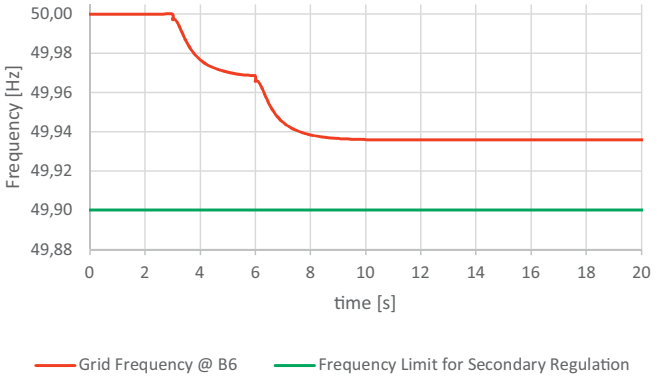


**Fig. 17.** Frequency trend at bus B6 in Scenario2a.

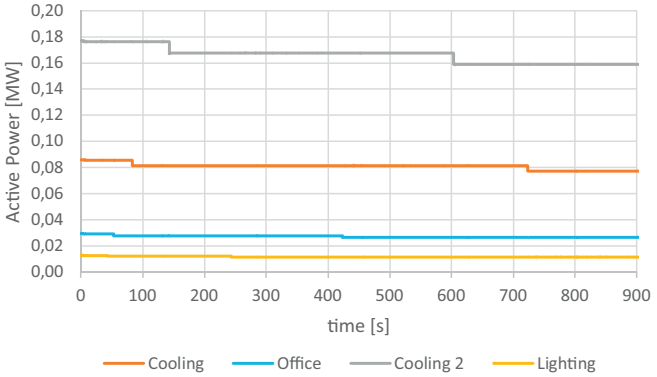


**Fig. 18.** DC loads power reduction in Scenario 2b.

Once that the steady-state is achieved after primary regulation, the frequency is 49.936 Hz with an error equal of 0.064 Hz. The error is bigger than the corresponding one in Scenario 1a; this is due to the lower abrupt generation detachment.

*4.3.2. Scenario 2b—DC secondary regulation by loads*

In this scenario the DC participates in secondary regulation by load power consumption modulation. The operation lasts 12 min and 30 s, therefore simulation time is 15 min (900 s).

Both the function blocks, "AD s1" and "AD s2" act on some DC loads by reducing their power demand during secondary regulation, as reported in Table 21.

The DC active power absorbed as primary frequency regulation effect (automatic loads regulation effect [48]) occurs until the 15th second. The DC active power input decrease from grid is 5.1 kW as shown in Fig. 18.

The DC power consumption slightly decreases as a consequence of the primary regulation effect, until the 15th second of the simulation. Then, in the connection lines *L 5-DC_A* and *L 5-DC_B*, the power flow decreases by 33.906 kW as shown in Table 22 due to DC loads modulation. The trends of the grid frequency is reported in Fig. 19.

**Table 22**
ΔP in the connection lines for scenario 2b.

| ΔP in L DC_A [kW] | ΔP in L DC_B [kW] | ΔP tot L DC [kW] |
|---|---|---|
| 19.247 | 14.659 | 33.906 |

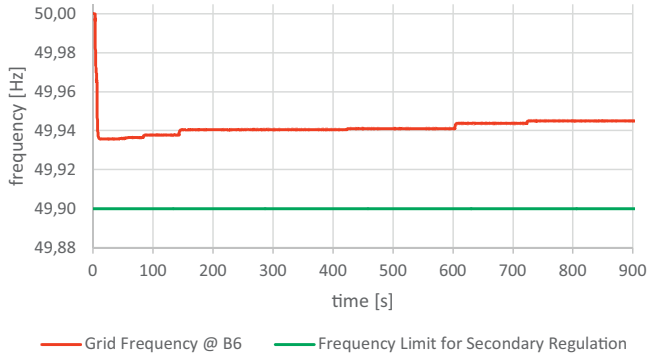


**Fig. 19.** Frequency trend at bus B6 during secondary regulation in Scenario 2b.

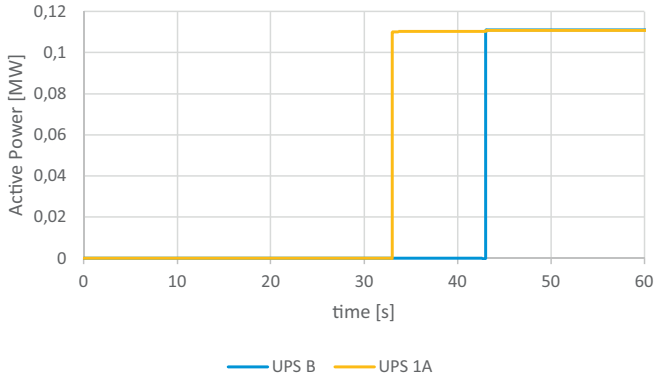


**Fig. 20.** Data centre UPS power supply in Scenario 2c.

**Table 23**
ΔP in connection line for scenario 2c.

| ΔP L DC_A [kW] | ΔP L DC_B [kW] | ΔP tot L DC [kW] |
|---|---|---|
| 105.0 | 105.5 | 210.5 |

*4.3.3. Scenario 2c—DC secondary regulation by UPSs*

In this scenario the DC participates in secondary frequency/energy regulation by switching on the UPS devices. The *Active Disturbance* function block turns on and activates the UPS energy delivery power as reported in Fig. 20. The active power input in the connection lines decreases substantially as shown in Table 23. The action lasts about 40 s, therefore the simulation time is 60 s.

Once the steady state is achieved, the grid frequency value is 50.002 Hz; the error is 0.002 Hz (−0.040% $f_n$) as shown in Fig. 21.

## 5. Results discussion

In the previous section, the DC participation to the secondary frequency regulation in two different scenarios has been simulated.

In Scenario 1, a 50% of power reduction for DFIG1 was supposed in two steps. After primary regulation the grid frequency is 49.980 Hz and the steady state error is 0.02 Hz. The secondary regulation, performed by the DC, was performed in two way. In the first case, we use the DC loads flexibility and, after the secondary regulation that has performed in 750 s, we obtain a grid frequency value of 49.989 Hz and the steady state error 0.01 Hz. In the second case we use the DC UPSs energy storage and, after the secondary

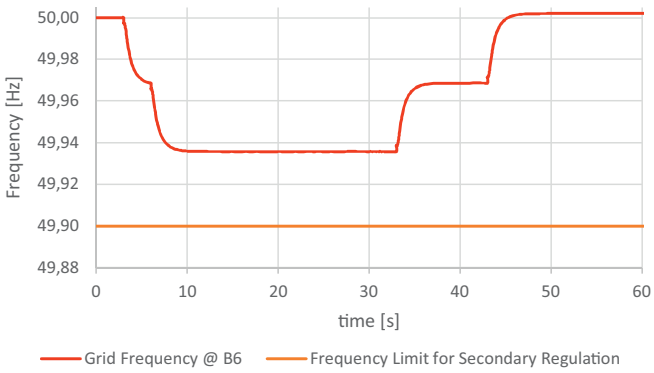


**Fig. 21.** Frequency trend at bus B6 in Scenario 2c.

**Table 24**
RES production variation.

| Facility involved | Reduction power | | Time [s] |
|---|---|---|---|
| | ΔP% | ΔQ% | |
| DFIG1 | −30% | −30% | 2 |
| | −20% | −20% | 6 |
| PV2 | −25% | −25% | 3 |
| | −25% | −25% | 10 |

regulation that has performed in 60 s, we obtain a grid frequency value of 50.046 Hz and the steady state error −0.046 Hz.

In Scenario 2, a 50% power reduction for PV2 was supposed in two steps too. After primary regulation the grid frequency is 49.936 Hz and the steady state error is 0.064 Hz. Also in this case, we have simulated the DC secondary regulation through the DC loads flexibility and thought the DC UPSs energy storage. In the first case, after the secondary regulation that has performed in 750 s, we obtain a grid frequency value of 49.945 Hz and the steady state error 0.055 Hz. In the second case, after the secondary regulation that has performed in 52.5 s, we obtain a grid frequency value of 50.002 Hz and the steady state error −0.002 Hz.

In both cases trough DC equipment, it has been possible to assist the grid during secondary frequency regulation. Furthermore, by using UPS, DC has been able to regulate by itself the grid frequency (obviously the RES facility had introduced small disturbances). DC collaboration in secondary frequency regulation, reduces the fluctuating work for conventional electrical power plants. The following tables synthetize the results of the simulations. The RES production variations are reported in Table 24, while Table 25 reports the frequency values and errors after the primary and the secondary frequency regulation, clearly showing the effects of the actions performed by the GDC.

It is important to underline that the GDC can participate to the secondary frequency regulation also combining the effect of its UPSs and of its interruptible loads. In this way, the contribution to the frequency restoration is even higher than that showed in the simulations. Moreover, the results obtained considering a reduction of the power produced by the RES facilities, can be generalized also to the case of increase of the MV power demand, as shown in Fig. 3. With regards to the expandability of the results of this study to much larger systems like the Italian transmission system, the DC can provide the same services also in these cases, in collaboration with the other consumers, generators and prosumers involved in the secondary frequency regulation. Of course, in such situations, a significant frequency adjustment will occur only thanks to the contribution of all the facilities involved in the regulation.

Some considerations are due on the influence of the models used for loads' simulation and for the secondary regulation on the obtained results. In particular, in this stage of our study, we used

**Table 25**
Frequency values and frequency errors.

| Sec. reg. | | Prim. reg. time frame [s] | f @ end reg1 [Hz] | Δf @ end reg1 [Hz] | Sec. Reg. time frame [s] | f @ end reg2 [Hz] | Δf @ end reg2 [Hz] |
|---|---|---|---|---|---|---|---|
| S | a) | 15 | 49.980 | 0.020 | – | – | – |
| 1 | b) | 15 | 49.980 | 0.020 | 750 | 49.989 | 0.010 |
| | c) | 15 | 49.980 | 0.020 | 60 | 50.046 | −0.046 |
| S | a) | 12.5 | 49.936 | 0.064 | – | – | – |
| 2 | b) | 12.5 | 49.936 | 0.064 | 750 | 49.945 | 0.055 |
| | c) | 12.5 | 49.936 | 0.064 | 52.5 | 50.002 | −0.002 |

a constant P, Q load model and a simplified scheme for secondary frequency regulation. Although these simplified assumptions do not influence the aim of the work, the presence of constant loads together with the absence of the AGC at the GDC, affect the trend of the frequency reported in Figures from 10 to 22 that do not show oscillations around the new frequency value after the regulation. Nevertheless the model implemented in NEPLAN is able to include both an AGC and frequency and voltage-dependent HV and MV loads (zip loads) as defined in Ref. [52].

## 6. Conclusion

The diffusion of RES plants connected to Medium and Low Voltage grids has been raising issues related to power reverse flow and to the grid stability due to natural unpredictability of RES. In order to promote the integration of RES and develop a new management strategy of the grid, ancillary services must be provided to the electrical power system.

This work describes the GDC contribution to secondary frequency/energy regulation when a wind farm output power decreases or a photovoltaic field power decrease occurs. Particularly, we focus on limiting the voltage violation frequency and, it is shown how GDCs can contribute to the rated frequency restoration in two different ways.

After the disturbance is applied, the TSO operates some control actions to regulate the frequency value in primary regulation. During secondary regulation this error shall be removed in order to reset the grid frequency value and take it close to 50 Hz. The contribution of DCs to restore the grid frequency has been implemented by means of DC loads shifting control and through the supply by DC UPS devices, causing the grid frequency to reach values closer to 50 Hz rated one.

Finally, it is underlined that in the case studies here presented, it has been assumed that GDCs are able to regulate their electricity profile according to the DSO request, although this is not what always happens in practice.

.As shown in Ref. [28], many of DR programs are not still available to GDC in markets yet and, anyway, they entail some risks for the DC. The presence of financial or degradation risks for the GDC is a challenge to face for increasing the participation of GDC to future DR programs.

Future works will study the business models that could regulate/remunerate the collaboration between GDCs and DSO.

## Acknowledgments

This work has been conducted within the GEYSER project, cofunded by the European Commission as part of the 7th Research Framework Programme (FP7-SMARTCITIES-2013).

## References

[1] J. Glanz, Power, pollution and the internet, NY Times 22 (09) (2016) 2012.
[2] G.F. Davies, G.G. Maidment, R.M. Tozer, Using data centres for combined heating and cooling: an investigation for London, ELSEVIER Appl. Therm. Eng. 94 (2015) 296–304.
[3] U.S. Environmental Protection Agency ENERGY STAR Program, Report to congress on several and data center energy efficiency, 2007.
[4] J.G. Koomet, Growth in Data Center Electricity Use 2005 to 2010, 1 August 2011 [Online], 2015, Available: http://www.analyticspress.com/datacenters.html. [Accessed 10 September 2015].
[5] National Institute of Standards and Technology, NIST Framework and Roadmap for Smart Grid Interoperability Standards, NIST Special Publication, 2010, 2017.
[6] X. Fang, S. Misra, G. Xue, D. Yang, Smart grid -the new and improved power grid: a survey, IEEE Commun. Surveys Tutorials 14 (4) (2012).
[7] D. of Energy—Office of Electricity Delivery & Energy Reliability, The smart grid: An introduction, 2011-05. [Online]. Available: http://energy.gov/oe/downloads/smart-grid-introduction-0.
[8] V. Depoorter, E. Oró, J. Salom, The location as an energy efficiency and renewable energy supply measure for data centres in Europe, ELSEVIER Appl. Energy 140 (2015) 338–349.
[9] C. Pfeiffer, Data Centers and the Smart Grid, 22 October 2012 [Online], 2014, Available: http://www.energymanagertoday.com/data-centers-and-the-smart-grid-086428/ [Accessed 3 June 2014].
[10] D. Gmach, Y. Chen, C. Hyser, Z. Wang, C. Bash, C. Hoover, S. Singhal, Integrated management of application performance, power and cooling in data centers, in: Network Operations and Management Symposium (NOMS), IEEE, Osaka, 2010.
[11] J. Heo, P. Jayachandran, I. Shin, D. Wang, T. Abdelzaher, X. Liu, On performance composition and server farm energy minimization application, Parallel Distrib. Syst. IEEE Trans. Parallel Distrib. Syst. 22 (11) (2011) 1871–1878.
[12] H. Lei, T. Zhang, Y. Liu, Y. Zha, X. Zhu, SGEESS: smart green energy-efficient scheduling strategy with dynamic electricity price for data center, ELEVIER J. Syst. Softw. 108 (2015) 23–38.
[13] M. Liu, A. Wierman, L.H. Andrew, E. Thereska, Dynamic right-sizing for power-proportional data centers, in: NFOCOM, Proceedings IEEE, Shanghai, 2011.
[14] GEYSER Project WebSite [Online]. Available: http://www.geyser-project.eu/. [Accessed 14 November 2014].
[15] G. Ghatikar, V. Ganti, N. Matson, M. Piette, Demand Response Opportunities and Enabling Tecnologies for Data Centers, 2012.
[16] A. Fernández-Montes, D. Fernández-Cerero, L. González-Abril, J.A. Álvarez-García, J.A. Ortega, Energy wasting at internet data centers due to fear, ELSEVIER Pattern Recogn. Lett. 67 (2015) 59–65.
[17] G. Ghatikar, M.A. Piette, S. Fujita, A. McKane, J. Han, A. Radspieler, K. Mares, D. Shroyer, Demand Response and Open Automated Demand Response Opportunities for Data Centers, Lawrence Berkeley National Laboratory, Berkeley, 2010.
[18] L. Rao, L. Liu, W. Liu, L. Xie, Optimization of distributed internet data centers in a multi-electricity-market environment, in: INFOCOM, Proceedings IEEE, San Diego CA, 2010.
[19] H. Xu, B. Li, Cost efficient datacenter selection for cloud services, in: 1st IEEE International Conference on Communications in China (ICCC), Beijing, 2012.
[20] P. Wendell, J.W. Jiang, M.J. Freedman, J. Rexford, Donar: decentralized server selection for cloud services, in: SIGCOMM '10 Proceedings of the ACM SIGCOMM 2010 Conference, New York, 2010.
[21] S. Govindan, D. Wang, A. Sivasubramaniam, B. Urgaonkar, Aggressive datacenter power provisioning with batteries, ACM Trans. Comput. Syst. (TOCS) 31 (1) (2013).
[22] B. Urgaonkar, M.J. Neely, A. Sivasubramaniam, Optimal power cost management using stored energy in data center, in: SIGMETRICS '11 Proceedings of the ACM SIGMETRICS Joint International Conference on Measurement and Modeling of Computer Systems, New York, 2011.
[23] Z. Liu, A. Wierman, Y. Chen, B. Razon, N. Chen, Data center demand response: avoiding the coincident peak via workload shifting and local generation, ELSEVIER Perform. Eval. 70 (10) (2013) 770–791.
[24] A. Wierman, Z. Liu, I. Liu, H. Mohsenian-Rad, Opportunities and challenges for data center demand response, in: International Green Computing Conference (IGCC), Dallas, TX, 2014.
[25] EDSO for Smatr Grids [Online], 2014, Available: http://www.edsoforsmartgrids.eu/. [Accessed 20 December 2014].
[26] J. Goiri, E. Haque, K. Le, R. Beauchea, T.D. Nguyen, J. Guitart, J. Torres, R. Bianchini, Matching renewable energy supply and demand in green datacenters, ELSEVIER Ad Hoc Netw. 25 (2015) 520–534.
[27] F. Niedermeier, W. Duschl, T. Möller, H. de Meer, Increasing data centre renewable power share via intelligent smart city power control, in: e-Energy

'15 Proceedings ofthe 2015 ACM Sixth International Conference on Future Energy Systems, New York, NY, 2015.
[28] E. Oró, V. Depoorter, A. Garcia, J. Salom, Energy efficiency and renewable energy integration in data centres. Strategies and modelling review, ELSEVIER Renew. Sustain. Energy Rev. 42 (2015) 429–445.
[29] C. Lo Prete, B.F. Hobbs, C.S. Norman, S. Cano-Andrade, A. Fuentes, M.R. von Spakovsky, L. Mili, Sustainability and reliability assessment of microgrids in a regional electricity market, ELSEVIER Energy 41 (2012) 192–202.
[30] Federal Energy Regulatory Commission, National Assessment of Demand Response Potential, 2009 [Online]. Available: https://www.ferc.gov/legal/staff-reports/06-09-demand-response.pdf.
[31] C.J. Tang, M.R. Dai, C.C. Chuang, Y.S. Chiu, W.S. Lin, A load control method for small data centers participating in demand response programs, ELSEVIER Future Gener. Comput. Syst. 32 (2014) 232–245.
[32] N. Chen, X. Ren, S. Ren, A. Wierman, Greening multi-tenant data center demand response, ELSEVIER Perform. Eval. 91 (2015) 229–254.
[33] R. Basmadjian, L. Müller, H. De Meer, Data centres' power profile selecting policies for demand response: insights of green supply demand agreement, ELSEVIER Ad Hoc Netw. 25 (2015) 581–594.
[34] EURELECTRIC, Eurelectric Termonology, [Online], 2014, Available: http://www.eurelectric.org/facts-terminology/terminology/networks-grids/networks/. [Accessed 20 12 2014].
[35] Intenational Council on Large Electric System (CIGRE), [Online]. Available: http://www.cigre.org. [Accessed 20 December 2014].
[36] IEEE Standards Coordinating Committee 21 on Fuel Cells, Photovoltaics, Dispersed Generation, and Energy Storage, IEEE Application Guide for IEEE Std 1547™, IEEE Standard for Interconnecting Distributed Resources with Electric Power Systems, IEEE, 2008.
[37] CEI, CEI 0-16—Regola tecnica di riferimento per la connessione di Utenti attivi e passivi alle reti AT ed MT delle imprese distributrici di energia elettrica, CEI, 2012-12.
[38] REserviceS—Economic grid support from variable renewables, [Online]. Available: http://www.reservices-project.eu/. [Accessed 20 December 2014].
[39] D. Aikema, R. Simmonds, H. Zareipour, Delivering ancillary services with data centres, ELSEVIER Sustain. Comput.: Inform. Syst. 3 (2013) 172–182.
[40] S.S. Oren, Design of ancillary service markets, in: Proceedings of the 34th Annual Hawaii International Conference on System Sciences, Maui, HI, USA, 2001.
[41] M.P. Ali, Ancillary Services, Definiscion, markets and practices in the world, IEEE/PES Trasmition and Distribution Conference and Exposition (2010), p. 5.
[42] S. Ali Pourmousavi, M. Hashem Nehrir, Introducing dynamic demand response in the LFC model, IEEE Trans. Power Syst. 29 (4) (2014) 1562–1572.
[43] V. Singh, P. Samuel, N. Kishor, Impact of demand response for frequency regulation in two-area thermal power system, Int. Trans. Electr. Energy Syst. 27 (2) (2017).
[44] TERNA, Partecipation to Frequency and Frequency Power Regulation, 2008.
[45] C. S. 0-21, National Technical Rule for the connection of active and passive users to the LV distribution grid—Italinan: Regola tecnica di riferimento per la connessione di Utenti attivi e passivi alle reti BT delle imprese distributrici di energia elettrica, 2014.
[46] University Of Washington—Electrical Engineering, Power System Test Case Archive [Online], 2015, Available: http://www.ee.washington.edu/research/pstca/. [Accessed 1 December 2015].
[47] A.G. Neplan, NEPLAN Smarter Tools, [Online], 2014, Available: http://www.neplan.ch/. [Accessed 1 September 2014].
[48] TERNA, Grid Code Annex 15: Participation to frequency and frequency-power regulation – in Italian: Codice di rete Appendice 15: Partecipazione alla regolazione di frequenza e frequenza-potenza, 2008.
[49] GRTN Direzione Rete Unità Regole e Sistemi, Criteri di taratura dei relè di frequenza del sistema elettrico, 2004.
[52] K. Hatipoglu, I. Fidan, MATLAB based GUI to investigate effect of voltage changes on static ZIP load model in a microgrid, in: IEEE SOUTHEASTCON, Lexington, KY, USA, 2014.